CMLS Cellular and Molecular Life Sciences

The coordination and function of the redox centres of the membrane-bound nitrate reductases

F. Blasco[a,*], B. Guigliarelli[b], A. Magalon[a], M. Asso[b], G. Giordano[a] and R. A. Rothery[c]

[a]Laboratoire de Chimie Bactérienne, IBSM, CNRS, 31 chemin Joseph Aiguier, F-13402 Marseille Cedex 20 (France), Fax + 33 04 91 71 89 14, e-mail: blasco@ibsm.cnrs-mrs.fr
[b]Laboratoire de Bioénergétique et Ingénierie des Protéines, IBSM, CNRS, 31 chemin Joseph Aiguier, 13402 Marseille Cedex 20 (France)
[c]Department of Biochemistry, 474 Medical Science Building, University of Alberta, Edmonton, Alberta T6G 2H7 (Canada)

Abstract. Under anaerobic conditions and in the presence of nitrate, the facultative anaerobe *Escherichia coli* synthesises an electron-transport chain comprising a primary dehydrogenase and the terminal membrane-bound nitrate reductase A (NarGHI). This review focuses on recent advances obtained on the structure and function of the three protein subunits of membrane-bound nitrate reductases. We discuss a global architecture for the Mo-bisMGD-containing subunit (NarG) and a coordination model for the four [Fe–S] centres of the electron-transfer subunit (NarH) and for the two *b*-type haems of the anchor subunit NarI.

Key words. Nitrate reductase; molybdenum cofactor; [Fe–S] centres; haems.

Nitrate reduction by *Escherichia coli*

In order to use nitrate as an electron acceptor, *E. coli* synthesises two distinct enzymes: a membrane-bound enzyme (nitrate reductase A, NarGHI) encoded by the *narGHJI* operon [1] and a soluble periplasmic nitrate reductase (NapAB) encoded by the *napFDAGHBC* operon [2]. A second membrane-bound nitrate reductase (nitrate reductase Z, NarZYV), encoded by the *narZYWV* operon is biochemically similar to NarGHI [3, 4]. Whereas NarGHI synthesis is induced by nitrate under anaerobic conditions, NarZYV is expressed at a cryptic level and may assist *E. coli* in the transition from aerobic to anaerobic respiration [3, 5]. Recently, Chang and co-workers [6] have provided evidence for RpoS-mediated regulation of the *narZYWV* operon, supporting a physiological role of this isoenzyme at the onset of the stationary growth phase in rich media. NapAB is mainly expressed in the presence of low concentrations of nitrate under both aerobic and anaerobic conditions, and its expression is suppressed at high nitrate concen-

trations [7–9]. Conversely, NarGHI is maximally expressed when nitrate concentration is elevated, and under these conditions becomes the predominant enzyme in *E. coli*. Thus, NapAB and NarGHI seem to function in different ranges of nitrate concentration in a complementary way to support anaerobic respiration on nitrate (see also article by Richardson et al.).

Of the two respiratory nitrate reductases, NarGHI is the more complex. Its general organisation is similar to that of other respiratory enzymes in which intramolecular electron transfer is coupled to the creation of a transmembrane proton electrochemical potential. NarGHI is a heterotrimer comprising a molybdenum cofactor-containing subunit [molybdo-bis(molybdopterin guanine dinucleotide), Mo-bisMGD. NarG, 139 kDa], an [Fe–S] cluster-containing electron-transfer subunit (NarH, 58 kDa) and a haem-containing membrane-anchor subunit (NarI, 26 kDa). These three subunits are arranged in two domains, with the NarG and NarH subunits constituting a cytoplasmic domain and the NarI subunit constituting a membrane-intrinsic domain required for attachment of the NarGH dimer to the cytoplasmic side of the cell membrane.

---

* Corresponding author.

NarG, the Mo-bisMGD-binding subunit of NarGHI

Towards a global architecture of NarG

The NarG subunit of NarGHI is a member of a super-family of oxidoreductase subunits with highly conserved organisation and sequence. During the last decade, the crystal structures of five bacterial Mo-bisMGD-containing enzymes have been reported: dimethylsulfoxide reductase from *Rhodobacter sphaeroides* [10] and *Rh. capsulatus* [11], formate dehydrogenase H from *E. coli* [12], trimethylamine *N*-oxide reductase from *Shewanella massilia* [13] and the periplasmic nitrate reductase, NapA, from *Desulfovibrio desulfuricans* [14]. All are globular proteins and are organised in four $\alpha\beta$ domains (I–IV) grouped around the Mo-bisMGD, and a funnel-shaped tunnel leads from the protein surface to the molybdenum atom. The Mo-bisMGD, which is ligated within the interfaces of the four domains through hydrogen bonds, salt bridges and van der Waals interac-

tions, is buried in the centre of the protein and extends through a major portion of the polypeptide. Today, no three-dimensional structure is available for a NarGHI type enzyme. Nevertheless, alignment of amino acid sequences of Mo-bisMGD-containing polypeptides, including NarG, with those of proteins with known structures shows extensive blocks of homology throughout the length of the protein, with the amino-terminal regions being the most highly conserved [15, 16]. The order of these blocks from amino- to carboxyl-terminus is constant and the residues involved in Mo and in Mo-bisMGD ligation are well conserved among these molybdoenzymes [10]. This strongly supports the idea that NarG has the same basic architecture as the other structurally characterised Mo-bisMGD-containing subunits. It is very likely to be organised in four $\alpha\beta$ domains grouped around the Mo-bisMGD. In taking the comparison a little further, we can guess that three segments constituted by residues 1–114, 795–823 and
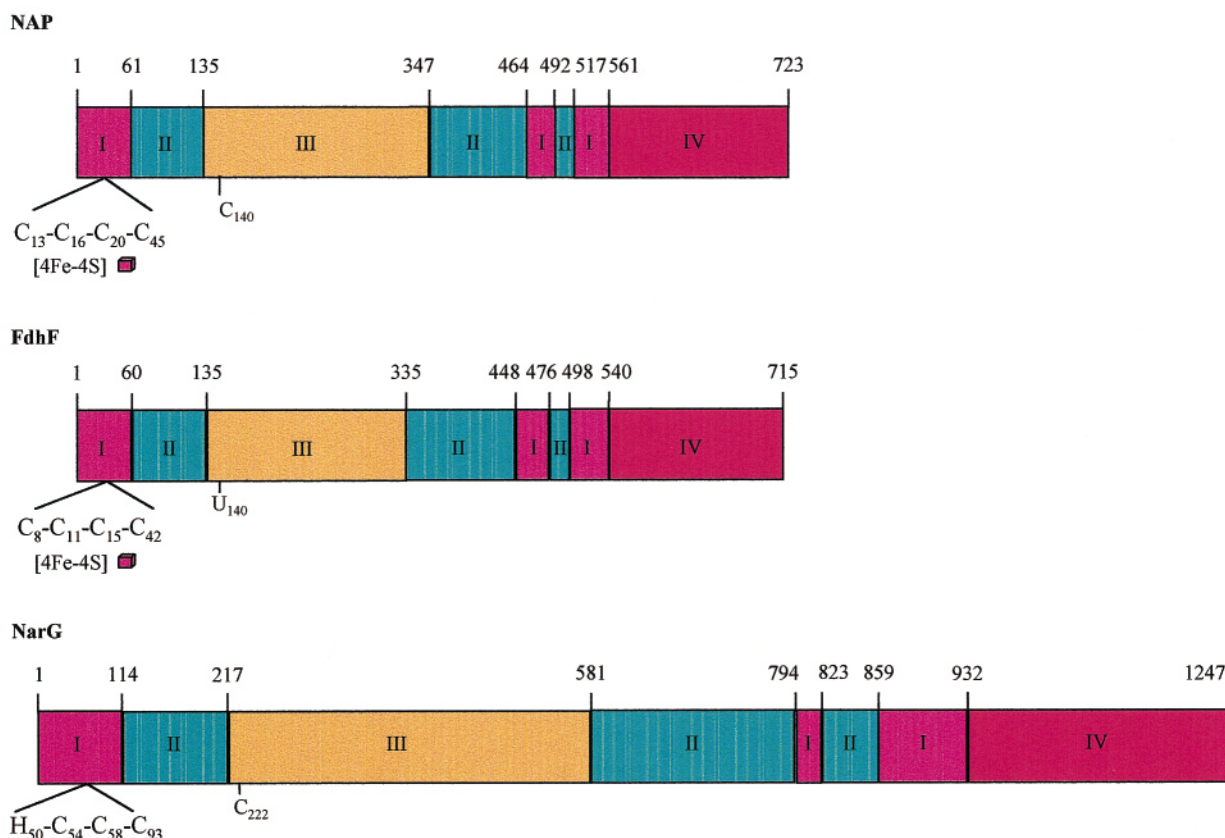

Figure 1. Schematic organisation of the four $\alpha\beta$ domains (I–IV) of NAP and FdhF deduced from crystal structures [12, 14]. Sequence homologies of NarG with those of NAP and FdhF support the idea that NarG shares their same basic architecture with four domains: domain I (in purple), domain II (in green), domain III (in orange) and domain IV (in red). The cysteine groups located at the N-terminus of the three subunits and involved in the coordination of a [4Fe–4S] centre in NAP and FdhF are indicated. The limits of each domain are numbered (amino acid number) starting from the NH$_2$-terminus. C_{140} in NAP, U_{140} (SeCys) in FdhF and probably C_{222} in NarG are involved in molybdenum coordination.

859–932 define the domain I of NarG. Domain II might also consist of three noncontiguous segments, including residues 115–217, 582–794 and 824–858. Domain III (residues 218–581) and domain IV (residues 933–1247) may comprise continuous stretches of amino acids. This overall organisation of NarG is tentatively depicted by figure 1 and compared with those of formate dehydrogenase [12] and NapA [14] deduced from X-ray crystallography.

The role of the N-terminal Cys group of NarG

The majority of the catalytic subunits of the bacterial molybdoenzymes show conserved Cys residues in their N-terminus arranged in a manner which is reminiscent of the Cys group involved in [4Fe–4S] cluster coordination in bacterial ferredoxins. These catalytic subunits have been classified into three types, I–III [17]. Type I enzymes contain four Cys residues, with the first three spaced in a manner similar to a bacterial ferredoxin eight-iron ($2 \times$ [4Fe–4S]) Cys group. Type II enzymes have three amino acids instead of two between the first and the second Cys residue, and type III enzymes do not contain the Cys region. *E. coli* NarGHI and dimethylsulfoxide reductase (DmsABC) are type II enzymes. Interestingly, the first Cys is replaced by a His in NarG (His50 in NarG). However, the presence of a His residue does not preclude the coordination of an [Fe–S] cluster, as such a residue provides a ligand to a [4Fe–4S] cluster in the [Ni–Fe] hydrogenase from *Desulfovibrio gigas* [18]. However, from site-directed mutagenesis and electron paramagnetic resonance (EPR) studies performed on the type II enzymes, NarGHI and DmsABC, it is not likely that the N-terminal Cys group located in their catalytic subunits ligates a [Fe–S] cluster [17, 19, 20]. In the case of DmsABC, it has been suggested [17] that the Cys motif of DmsA is a degenerate Cys group that has lost the capability to bind a [4Fe–4S] cluster during evolution.

The presence of a His residue instead of a Cys in NarG raises the question of its function. Substitution of His50 by Ser or Cys prevents (H50S) or restrains (H50C) Mo-bisMGD insertion [19]. By considering the three-dimensional structure of *E. coli* formate dehydrogenase H enzyme (FdhF), and assuming that the global folding of NarG and FdhF are similar (fig. 1), we can assume that the NarG His50 residue belongs to a domain that lies close to the Mo-bisMGD in the folded enzyme. Its substitution by a Ser or a Cys residue could then introduce sufficient local structure distortion or hydrogen-bonding disorder to prevent or restrain cofactor insertion.

Mutation of the Cys residues located at the N-terminus of NarG eliminates enzyme activity [unpublished results]. Taken together with results obtained for

DmsABC [17, 21], these data suggest that functional electron transfer in NarGHI-type enzymes requires the integrity of the N-terminus Cys group of their catalytic subunits.

Catalytic mechanism

Based on sequence homology and the reaction catalysed, the molybdoenzymes have been classified into three families, exemplified by xanthine oxidase, sulphite oxidase and DMSO reductase [22]. With the exception of the eukaryotic assimilatory nitrate reductases (see article by Campbell), the dissimilatory enzymes have been placed in the DMSO reductase family, where members are distinguished by bis-dithiolene coordination of the molybdenum. The Mo(V) state of the molybdenum cofactor in the NarGHI-type enzymes exhibits unique EPR properties in comparison with their periplasmic and assimilatory cytoplasmic counterparts. A key difference between the Mo(V) signals relates to the origin of the proton responsible for their hyperfine splitting. For example, the EPR Mo(V) signals from *E. coli* NarGHI undergo an acid-base transition between a low-pH and a high-pH form, the low-pH form being characterised by a strong hyperfine splitting due to a solvent-exchangeable proton [23, 24]. It has been previously suggested that only the low-pH Mo(V) form is catalytically relevant [23]. However, the high-pH and the low-pH forms of the Mo(V) are both involved during enzyme turnover [19]. Whereas EPR analysis of the wild-type NarGHI shows that the two Mo(V) forms represent a conjugate acid/base pair with a pK_V of 7.4, the pK_V value is lowered to 6.8 in a H50C mutant enzyme [19]. Such a pK_V shift could result from a perturbation of the hydrogen-bonding network around the molybdenum atom. The His residue is thus most likely involved in stabilisation of the hydrogen-bonding network of the molybdenum cofactor, since the replacement of the sulphydryl group (H50C) by a hydroxyl one (H50S) is sufficient to preclude the binding of the molybdenum cofactor. At high pH, similar midpoint potentials were found for the Mo(VI)/Mo(V) and Mo(V)/Mo(IV) couples between the wild-type and H50C mutant enzymes. Surprisingly, at low pH, no oxidation of the Mo(V) state to the Mo(VI) state was observed even at potentials as high as $+400$ mV, which shows that the midpoint potential of the low-pH Mo(V)/Mo(VI) couple is significantly higher than this value. The inability of the low-pH Mo(V) form to undergo final oxidation to Mo(VI) would prevent the reduction of nitrate to nitrite ($E_{m,7} = +420$ mV), a two-electron and two-proton process. Overall, the high-pH and the low-pH forms of the Mo(V) might both be involved during catalytic turnover of the enzyme. A model for the reoxidation of the molybdenum atom by

nitrate during the catalytic cycle has been proposed [19]. One of the key features of this model is that one of the two protons involved in the nitrate reduction might be the one associated with the acid-base transition of the cofactor. Modification of the pK_V value in the H50C mutant enzyme changes the interconversion rate between the low-pH and high-pH forms of the Mo(V), which as a consequence could affect the rate of the catalytic cycle. In this model, one of the two protons involved in reduction of nitrate is missing. A protonable amino acid residue lying in the vicinity of the molybdenum cofactor could provide this proton.

Molybdenum cofactor insertion

The NarJ polypeptide (26.5 kDa) encoded by the narGHJI operon is not part of the final enzyme but is required for nitrate reductase activity [25–28]. NarGHI-type enzymes from *Bacillus subtilis* [29] and *Thermus thermophilus* [30] require such a protein, as related genes have been identified in their respective operons. Liu and DeMoss [31] proposed that the NarJ protein is a specific chaperone required for the assembly of NarGHI. Recent data have converged to show that NarJ is involved in the acquisition of Mo-bisMGD by NarGH prior to its attachment to NarI [28, 32].

The question as to the exact nature of the changes induced in NarG by NarJ still remains to be elucidated. The crystals of several molybdoenzymes indicate that the cofactor is buried within the mature proteins. The role of NarJ might, therefore, be to hold apo-NarGH in a cofactor-insertion-competent conformation. This final step is probably mediated by a carrier protein [33, 34], which delivers the cofactor to the NarGHJ ternary complex. In some cases, assembly of metallocentres appears to be a complex process requiring the action of several accessory gene products catalysing a whole maturation cascade in a specific order [35–38]. The presence of specific chaperones for metalloenzymes seems to be widespread in bacteria, although the operons of several molybdoenzymes, including formate dehydrogenase N [39], DmsABC [40, 41] and polysulphite reductase [42], do not encode NarJ-type proteins. It would certainly now be worth investigating whether proteins encoded by other transcriptional units might also be involved in cofactor acquisition by these molybdoenzymes via processes similar to those involving NarJ in the maturation of NarGHI.

The electron-transfer subunit, NarH

The [Fe–S] clusters of NarGHI: redox and spectral properties

The presence of [Fe–S] clusters in NarGHI from *E. coli* has been recognised for many years [23], but the determination of their nature and number had to await the beginning of 1990s, when quantities of enzyme large enough for detailed biophysical characterisations could be obtained. EPR spectroscopy was largely used in these studies since it gives a distinct signature for each centre of the enzyme. Four [Fe–S] clusters have been identified in the soluble NarGH complex. They belong to two classes with markedly different redox properties [43]. The high potential class contains a $[3Fe–4S]^{1+,0}$ and a $[4Fe–4S]^{2+,1+}$ cluster, which are EPR detectable in their oxidised and reduced states, respectively. The $[3Fe–4S]^{1+}$ cluster has a nearly isotropic EPR signal around $g = 2.0$ with very broad lines (fig. 2a), whereas the $[4Fe–4S]^{1+}$ cluster exhibits a rhombic signal at $g = 2.04$, 1.95 and 1.87. Both clusters are characterised by very fast relaxation properties, their EPR signals being unsaturated at 15 K with 100 mW microwave power. In the soluble NarGH dimer, their redox potentials are unusually high, $+80$ and $+60$ mV for the $[4Fe–4S]^{2+,1+}$ (centre 1) and $[3Fe–4S]^{1+,0}$ (centre 2) clusters, respectively, close to the values usually measured for the $[4Fe–4S]^{3+,2+}$ centre from high potential [Fe–S] proteins. Interestingly, although these two centres are coupled by an anticooperative redox interaction of about 50 mV [43], no magnetic couplings are observed between them, suggesting that they may be distant in the enzyme. The low potential class contains two $[4Fe–4S]^{2+,1+}$ clusters with redox potentials of -200 mV (centre 3) and -400 mV (centre 4) in the soluble NarGH complex. Reduced centre 3 has a broad rhombic EPR signal with slower relaxation properties than the high potential clusters. However, due to their spin-spin interactions with reduced centres 1 and 2, the EPR spectral contributions of centres 3 and 4 cannot be clearly identified, and the fully reduced nitrate reductase has a broad and relatively featureless spectrum (fig. 2d) that is reminiscent of that of other multicentre [Fe–S] enzymes [44].

Based on the midpoint potentials obtained for the [Fe–S] clusters of the soluble NarGH dimer, only the high potential clusters were initially considered to be involved in electron-transfer from quinol ($E_m = -80$ mV) to nitrate ($E_m = +420$ mV). Recently, overexpression of the whole NarGHI enzyme in *E. coli* enabled reinvestigation of the redox properties of the [Fe–S] clusters in the membrane-bound NarGHI holoenzyme [19, 32]. These were found to be significantly different from those of the NarGH dimer. For instance, midpoint potential values of $+180$ mV for the $[3Fe–4S]^{1+,0}$ cluster (centre 2), and $+130$, -55 and -420 mV for centres 1, 3 and 4, respectively, are obtained for membrane-bound NarGHI [32]. It is likely that these variations are not due to important conformational changes of the NarGH complex, but rather to exposure of the clusters to the aqueous milieu. The large increase ob-
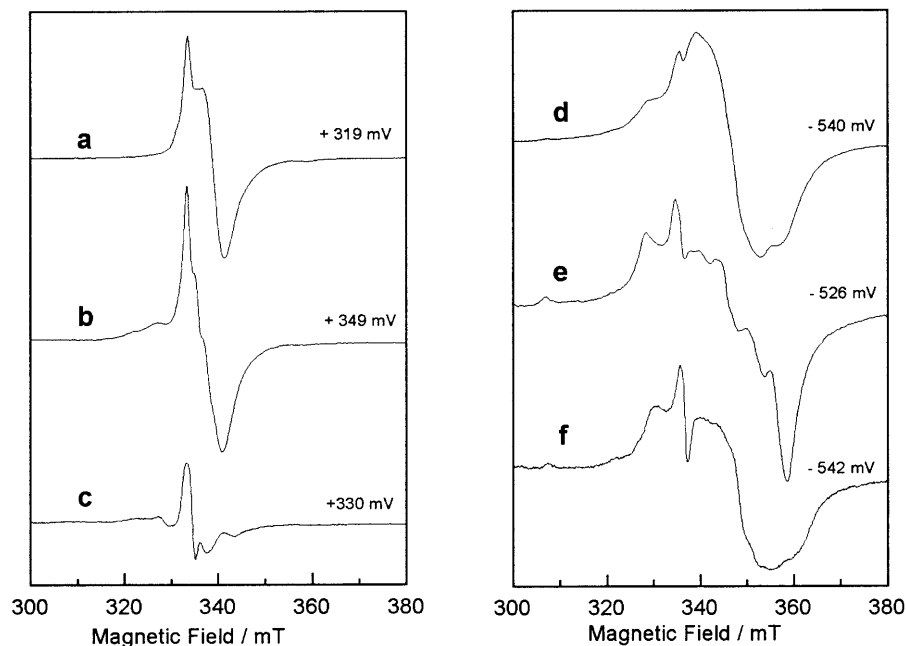
Figure 2. EPR spectra of overexpressed NarGHI nitrate reductase in *E. coli* inner membranes. (*a,d*) wild-type NarGHI enzyme; (*b,e*) NarGH^{C247D}I variant; (*c,f*) NarGH^{W220C}I variant. Experimental conditions: temperature, 15 K; microwave power, 100 mW at 9.416 GHz; modulation amplitude, 0.5 mT at 100 kHz. The residual signal visible in (*c*) probably arises from a membrane-bound Ni–Fe hydrogenase.

served in the membrane-bound enzyme for the E_m value of centre 3 suggests that it may undergo oxidation-reduction during enzyme turnover. However, the physiological significance of the spreading of the [Fe–S] redox potentials over a 650-mV range remains to be understood.

Coordination scheme of the [Fe–S] clusters
Sequencing the *narGHJI* operon led us to identify in the polypeptide sequence of NarH, four Cys groups similar to those binding [Fe–S] clusters in ferredoxins [1]. In order to determine the binding site of each cluster, a strategy based on their selective removal by substituting their putative ligands was extensively used. In ferredoxins, each [4Fe–4S] cluster is bound by the first three Cys of one group and by the fourth Cys of the second. Therefore, the first and fourth Cys of each Cys group of NarH were systematically replaced by Ala and Ser, and mutated enzymes were overproduced as soluble NarGH complexes. Centre 1 could be easily eliminated by substituting Ala either for the two first Cys residues of group I, or for the fourth Cys of group IV, with almost no change of the spectral and redox properties of the other clusters [45, 46]. The binding of this [4Fe–4S] centre made it possible to rule out a NarH organisation model resulting from a simple duplication of a 2 ×

[4Fe–4S] ferredoxin structure. However, in a number of mutant enzymes, the structural influence of mutations was so severe that no metal cofactors could be inserted [47]. The influence of point mutations affecting the low potential clusters, like C26A and C184S, were difficult to interpret since, due to spin-spin interactions, their effects could not be clearly identified by EPR. This led to ambiguities about the cluster organisation in NarH, and two coordination models were proposed for the low-potential [4Fe–4S] centres [46]. In these models, and by analogy with ferredoxins, the [3Fe–4S] cluster was assumed to be bound by Cys group III in which the second Cys is lacking, being replaced by Trp (W220). However, it should be kept in mind that there is no direct relationship between the sequence of the Cys group and the nature of the bound cluster; a [3Fe–4S] can be bound by a consensus motif of 4 Cys residues, as in ferredoxin I from *Azotobacter vinelandii* [48], and conversely, a [4Fe–4S] can have noncysteinyl coordination [49]. Hence, direct evidence for the binding of centre 2 by Cys group III was required, but attempts at removing this [3Fe–4S] cluster selectively, or at converting it in a [4Fe–4S] cluster through a W220C substitution were unsuccessful in the NarGH complex [47].
Mutagenesis experiments carried out on the ferredoxin-like PsaC protein of Photosystem I (PSI) have been found to give different results, depending on the bound

or unbound state of PsaC to the PSI core [50, 51]. Thus, some mutations of the second Cys in the Cys motifs of PsaC led to [4Fe–4S]→[3Fe–4S] conversion in soluble PsaC protein, whereas the [4Fe–4S] clusters were maintained when mutated PsaC was docked to the PSI complex. These results prompted us to reinvestigate some mutation effects in membrane-bound NarGHI holoenzyme to avoid possible artefacts arising from the solubilisation of the NarGH complex. Recent studies have focused on modifications of the second residue of each Cys group to induce [4Fe–4S]↔[3Fe–4S] inter-conversions, which preserve the structural role of the cluster [F. Blasco, M. Asso and B. Guigliarelli, unpublished work]. Such an approach has required the development of expression systems providing a high level of NarGHI overexpression in order to enable the EPR analysis of *E. coli* membrane fractions in spite of the presence of other [Fe–S] enzymes [19]. Some results are illustrated in figure 2. EPR spectra of wild-type membrane-bound NarGHI in its fully oxidised, and fully reduced states show the [3Fe–4S]$^{1+}$ cluster signal (fig. 2a) and that arising from the three spin-coupled [4Fe–4S]$^{1+}$ clusters (fig. 2d). In the C247D mutant, the EPR spectrum given by the fully reduced enzyme is strongly modified, becoming more similar to that exhibited by the wild-type enzyme at higher potentials (fig. 2e). Moreover, in the oxidised state, the [3Fe–4S]$^{1+}$ signal of the mutant appears to be composite and more intense (fig. 2b). The spin intensity ratio between these two states changes from 1:3 in the wild-type enzyme to 2:2 in the C247D mutant. This clearly shows that the lowest potential [4Fe–4S] cluster is converted into [3Fe–4S] centre by the mutation and unambiguously confirms the coordination of centre 4 by Cys group IV. Conversely, when the W220C mutant is expressed in *E. coli* membranes, the [3Fe–4S]$^{1+}$ signal is no longer observable (fig. 2c). In the fully reduced state, this mutant gives a broad EPR signal (fig. 2f), similar to that obtained with the wild-type enzyme. Thus, as observed for the PsaC protein of PSI, the influence of the W220C mutation is different in the soluble NarGH complex and in the membrane-bound NarGHI enzyme. In the former case, the [Fe–S] clusters of the complex are unmodified, whereas in the latter, centre 2 disappears. This cluster is likely converted to a [4Fe–4S] cluster. Taken together, these results enable an unambiguous determination of the binding sites of the four [Fe–S] clusters in NarH, which leads to the coordination scheme shown in figure 3a.

On the functional role of [Fe–S] centres

In the coordination scheme of figure 3a, the [Fe–S] centres are associated in two pairs, containing a high potential and a low potential cluster each. Mutagenesis

experiments have shown that the selective removal of one of the high-potential clusters, whether centre 1 or centre 2, is accompanied by a strong decrease of the enzymatic activity ($\sim 90\%$). This indicates that these centres play an important role in the intramolecular electron transfer; however, they are not absolutely required since the mutated enzymes remain $\sim 10\%$ active. Assuming that the low-potential clusters play no redox role, this favours a model in which centres 1 and 2 are involved in two parallel electron pathways towards the Mo cofactor [46]. As no magnetic interactions have been detected between the Mo centre and centres 1 and 2, this suggests that these metal centres may be distant in the enzyme, which raises the question about the presence of additional intermediate redox centres [52]. The presence of a conserved Cys group in NarG, homologous to that binding the [4Fe–4S] cluster of periplasmic nitrate reductase, led to the proposal that a fifth cluster could be present between the [Fe–S] clusters of NarH and the Mo cofactor [53]. To date, no evidence for the existence of such a fifth cluster has been found [19]. However, the presence of a [4Fe–4S] cluster with a very low redox potential (less than -600 mV) and not detected by EPR cannot be excluded. In this context, it is interesting to compare the [Fe–S] cluster organisation in NarH with those found for other [Fe–S]-containing oxidoreductases and to reconsider the putative function of the low-potential [Fe–S] centres of the NarH subunit.

In the last few years the three-dimensional structure of bacterial [Fe–S] enzymes have been obtained by X-ray crystallography, namely [Ni–Fe] hydrogenase [18] and fumarate reductase (FRD) [54, 55]. These enzymes contain three [Fe–S] clusters that are nearly aligned in the structure, providing a plausible electron-transfer pathway. In FRD and [Ni–Fe] hydrogenase the median cluster has a potential much lower or higher than the two other centres (fig. 3b and c), which appears to be kinetically very unfavourable for electron transfer. Strikingly, the conversion by mutagenesis of the median [3Fe–4S] centre into [4Fe–4S] cluster in Ni–Fe hydrogenase from *Desulfovibrio fructosovorans* was accompanied by a 300-mV lowering of its midpoint potential, but had only a slight effect on the enzymatic activity [56]. Several hypotheses have been proposed to interpret these observations: (i) The median cluster is located on the electron-transfer pathway but has no redox role. This would imply a direct electron exchange between the two other centres distant of about 20 Å. (ii) Despite endergonic steps, the intramolecular electron exchange is not rate limiting for the enzymatic reaction [57]. (iii) Midpoint potentials, as measured by equilibrium redox titrations, are macroscopic quantities that are not relevant to describe dynamic processes such as intramolecular electron transfer in multicentre enzymes. In these
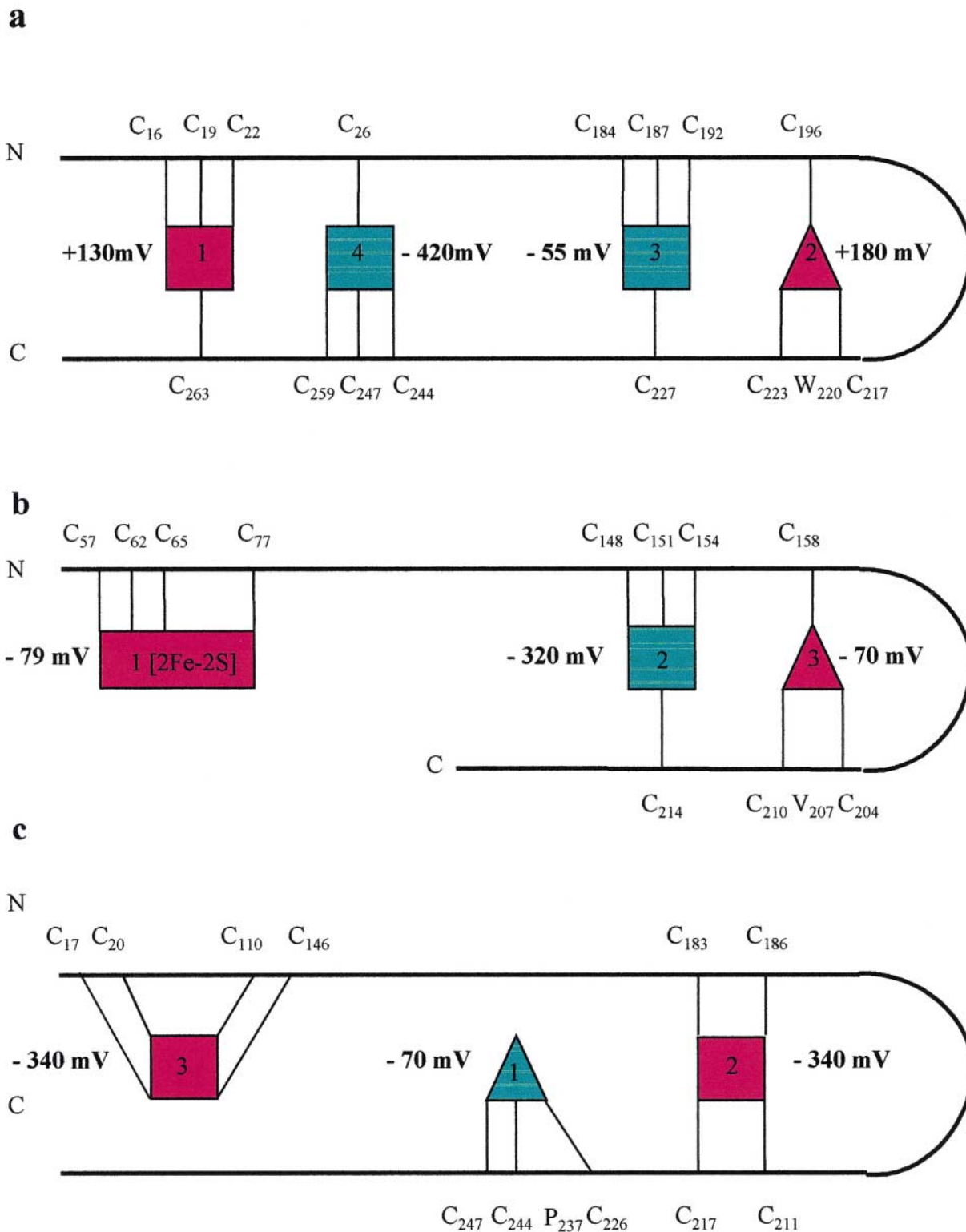
a

b

c

Figure 3. Schematic representation of the [Fe–S] cluster coordination in (*a*) *E. coli* NarGHI nitrate reductase, (*b*) *E. coli* fumarate reductase, (*c*) *D. gigas* [Ni–Fe] hydrogenase. Triangles correspond to [3Fe–4S] clusters and squares to [4Fe–4S] or [2Fe–2S] clusters.

```
              1         11        21        31        41        51        61        71        81
nari_ecoli    ~~~~~~~~~~ ~~~~MQFLNMF FFDIYPYIAG AVFLIGSWLR YDYGQYTWRA ASSQMLDRKG MNLASNLFHI GILGIFVGHF FGMLTPHWMY
narv_ecoli    ~~~~~~~~~~ ~~MIQYLNVF FYDIYPYICA TVFFLGSWLR YDYGQYTWRA SSSQMLDKRG MVIWSNLFHI GILGIFFGHL FGMLTPHWMY
nari_pseud    ~~~~~~~~~~ ~~~~MSTNLL FFGIYPYVAL LICLVGSWAR FDLSQYTWKA GSSQMLSKKG MRVYSNLFHV GVLFILAGHF VGLLTPASVY
nari_parc     ~~~~~~~~~~ ~~~~~~MNNF LFGIYPYIAĪ TVMLLGSIIR YDQDPFSWKS KSSQILRRRQ ṛVIGSVLFHV GVLVIFFGHL VGLLTPIAVF
nari_bacsu    ~~~~~~~~~~ ~~~~~MSGQI LWGIMPYIVL TIFIGGHIYR YQHDQFGWTA KSSELLEKKK LAAGSTLFHW GLLCVVGGHV MGILIPEGVY
nari_staph    ~~~~~~~~~~ ~~~~~MLNQF LWVIYPYLCV AIFIIGHIAR YRYDQFSWTA KSSEFIEKKR LKWGSLLFHL GIIPVAAGHF VGLVIPAAWL
nari_myco     ~~~~~~~~~~ ~MAVLDLVEI FWDAAPYVVV AIAVVGTWWR YRYDKFGWTT RSSQLYESRL LSIGSPMFHF GSLLVIMGHV MGLFIPDSWT
nari_strep    ~~~~~~~~~~ ~~~~~~MNVF LWGVLPYAAF ALLIAGLVWR HRYDRFGWTT RSSQIYESKL LNIASPVFHY GILFVLAGHL IGLFIPASWT
nari2_strep   MSATPAAPAP LAAASGSVLL LWVAVPYICL AVFAVGHVWR YRQDQFGWTS RTTQLLERRW LRWGSPLFHL GAFMVIAGHV VGLAVPASWT
nari_therm    ~~~~~~~~~~ ~~~~MKWNAA LFGVFPYIAL TLAVAVTAYR MVYRPFSVSA QSSQLLEQKR LFFGSTAMHW GLVIVLLGHL LALLLVPKGLL
Consensus     ---------- -------N-F LWGIYPYIA- A-F--G---R Y-YDQF-WTA -SSQ-LE-K- L--GS-LFH- G-L-V--GH- -GLL-P----
                          P               1                        C                      2               P


              91        101       111       121       131       141       151       161       171
nari_ecoli    EAW.LPIEVK QKMAMFAGGA SGVLCLIGGV LLLKRRLFSP RVRAT.TTGA DILILSLLVI QCALGLLTIP F.SAQHMDGS EMMKLVG.WA
narv_ecoli    AWF.LPVAAK QLMAMVLGGI CGVLTLIGGA GLLWRRLTNQ RVRAT.STTP DIIIMSILLI QCLLGLSTIP F.SAQYPDGS EMMKLVG.WA
nari_pseud    HHL.ISTENK QLLAMVSGGF FGVLCFIGLS GLILRRLTDA RVRAT.GNAS DLMILLVLYA QLILGLSTIV A.STHHMDGS VMVMLAE.WA
nari_parc     DALGISHGAK QVLAMTAGGI AAVMALVGGG MLLHRRLTDP RVLAAHTTLA DTGILALLVA QLVLGLMTIL V.SMQHLDGH EMTRLMS.WA
nari_bacsu    ASLGISEHMY HKMAIGAGLP AGIAACTGLV ILTYRRLFDK RIRKT.SSPS DILTLLLLLF MMLSGVAATF L..NIDSKGF DYRTTVGPWF
nari_staph    EGMGVNNHIY HIGAVYIGSL FGFMVLIGMI LLTYRRVSIK NIRRL.SSAS DMVVNFFLLV IICMGLYSTL V.TNAISPEF DYRQTISIWF
nari_myco     RAFGMSDHLY HLQALLLGAP AGFATLLGIG LLIYRRRIQT PVWLA.TTRN DKLMYLVLVC AIVAGLACTL MGATHEGDMH DYRRSVSVWF
nari_strep    QSIGISEHAY HLFSLYGGTV SGVLAVAGIG MLVYRRRTNA PVFRA.TTAN DKLMYVFLLG ALLLGMIAKL SDTS..GNGY DYRSTIAPWS
nari2_strep   EAAGVDEHTY HTTAVWAGSV AGVAMVAGLG MLCARRLLTR RIRLG.TDRS DKVLFPLLSA TVLLGITATA A.HNVFGAGY DYRSTVSVWF
nari_therm    LWNAVPLRLY LLEITGLG.. LGLWALFGTY VLLARRIAVA RVRAA.STPM DYLVLVVVFV SALTGVLTAV LYRY...GSF WFPAVMTPYL
Consensus     ---G-S-H-Y HL-A---G-- -GV--L-G-- -L--RRL--- RVRA--TT-- D-L-L--L-- --LLGL-T-- -------DG- DYR--V--W-
                P                          3                        C                      4                    P


              181       191       201       211       221       231       241       251       261
nari_ecoli    QSVVTFHG.G ASQHLDGVAF IFRLHLVLGM TLFLLFPFSR LIHIWSVPVE YLTRK.YQLV RARH~~~~~~ ~~~~~~~~~~ ~~~~~~~
narv_ecoli    QSIVTFRG.G SSEMLNGVAF VFRLHLVLGM TIFLLFPFTR LVHVWSAPFE YFTRR.YQIV RSRR~~~~~~ ~~~~~~~~~~ ~~~~~~~
nari_pseud    QAIVTLRPLA AAEAIAPVGL VYKLHVGLGL TLFVLFPFTR LVHIVSAPVW YLGRR.YQIV RQKRP~~~~~ ~~~~~~~~~~ ~~~~~~~
nari_parc     QGIVYFR.AG AADHLVGVHW LFKLHILLGL TIFLLFPFTR LVHMISAPVR YLWRPGYQYV RTKRQPAKRH PAE~~~~~~~ ~~~~~~~
nari_bacsu    REIVLFRPD. .ASLMESVPL WFKFHIVIGY VVFILWPFTR LVHVFSLPLK YLTRS.YVVY RKRS~~~~~~ ~~~~~~~~~~ ~~~~~~~
nari_staph    RHLFTFNPN. .ASLMTNVPW SFKLHIFLGF SIFALWPFTR LVHVWSVPLS YANRS.YIIY RKNKART~~~ ~~~~~~~~~~ ~~~~~~~
nari_myco     RSIWMLAPR. .GDLMAQATL YYQVHVLIAL ALFALWPFTR LVHAFSAPIA YLFRP.YIVY RSREVAAKHE LIGSAPRRRG W~~~~~~~
nari_strep    RSLFTLNPK. .TELMAGVPV LYHVHAVVGM VLIALVPYTR LVHMFSAPLQ YLTRP.YVVY RSRD....PR QLGPRPDRRG WERAGS~
nari2_strep   RGLFTLQPQ. .PEAIAGAPM LFQLHALSAC LLFAVWPFTR LVHVWSAPVG YLVRP.YVVY RRRAAAP.GR TAGPARRDRH PV~~~~~
nari_therm    WSVLTLNPR. .PELLQDLPF WTKLHVFNFW LFLALFPFSR LVHIITVPLG YVVRPWQIVV WVRNWRGEL~ ~~~~~~~~~~ ~~~~~~~
Consensus     RSIVT--P-- --EL--GVP- -FKLH--LG- -LFALFPFTR LVH--SAP-- YL-RP-Y-V- R-R------- ---------- -------
                          P                        5                        C
```

Figure 4. Sequence alignment of NarI subunits. NarI proteins were identified using the Netblast program of the Wisconsin Sequence Analysis Package (Version 9.1, Genetics Computer Group (GCG), Madison WI). Sequences were aligned using the Clustalw alignment algorithm [61]. *Key*: nari_ecoli, *E. coli* NarI (accession no. P11350); narv_ecoli, second *E. coli* NarI (P19316); nari_pseud, *Pseudomonas aeruginosa* NarI (Y15252); nari_parc, *Paracoccus denitrificans* NarI (S61309); nari_bacsu, *Bacillus subtilis* NarI (P42177); nari_staph, *Staphylococcus carnosus* NarI (AAC82545); nari_myco, *Mycobacterium tuberculosis* NarI (Z95584); nari_strep, *Streptomyces coelicolor* NarI (AL031515); nari2_strep, second *Streptomyces coelicolor* NarI (CAB53443); nari_therm, *Thermus thermophilus* NarI (Y10124). Putative transmembrane segments [62] are underlined, and absolutely conserved residues are in bold type. *P*, periplasmic loop; *C*, cytoplasmic loop.

systems, microscopic potentials taking into account intercentre redox cooperativity should be considered in the kinetic analysis [49]. Experimental data favouring one of these hypotheses are still lacking. However, these observations suggest that the low midpoint potentials measured in NarGHI do not necessarily mean that the corresponding [Fe–S] centres are excluded from the electron-transfer pathway. Despite the determination of the binding sites of the [Fe–S] clusters in NarH, the relative arrangement of the two pairs of clusters (centres 1, 4 and 3, 2) is not known. Kinetic studies based on stopped-flow experiments and new insights provided on the structural organisation of the prosthetic groups by EPR analysis of spin-spin couplings and X-ray crystallography would be a promising way to understand the role of each centre in the enzyme.

NarI, the haem-containing membrane-anchor subunit of NarGHI

NarI (225 amino acid residues, 26 kDa) anchors NarGH to the inner surface of the cytoplasmic membrane [1, 58–60]. It is also the site of quinol binding and oxidation, and provides an electron-transfer conduit from this functionality to the [Fe–S] clusters of NarH. Electron transfer out of NarI is mediated by two haems, one of relatively low midpoint potential E_m (haem b_L), and one of relatively high E_m (haem b_H) [58–60].

Overall structure and haem composition

A NarGHI-type nitrate reductase has been identified in a range of bacterial species. Figure 4 shows 10 NarI sequences aligned using the ClustalW alignment al-

gorithm [61]. The diversity of the sequences provides a convenient filter for the identification of important amino acid residues. Hydropathy analyses suggest the presence of five transmembrane helices (TM1–TM5), with a periplasmic amino-terminus and a cytoplasmic carboxy-terminus [62]. Figure 5a shows a plot of the overall sequence similarity in the alignment of figure 4 versus residue position in combination with the proposed transmembrane topology of NarI (fig. 5b). Within the proposed TM segments, similarity peaks are located in TM1, TM2 and TM5. The observed similarity in TM2 and TM5 is consistent with these helices being the location of the four His residues that coordinate the two haems [58, 60]. The distribution of the similarity scores within the membrane-extrinsic loops can provide information on the transmembrane topology of NarI. Within the NarI sequences, above average similarity is observed in loop TM1–TM2 (putative cytoplasmic) and after the end of TM5 (putative cytoplasmic). Below average similarity is observed in loops TM2–TM3 (putative periplasmic), TM3–TM4 (putative cytoplasmic) and TM4–TM5 (putative periplasmic). However, in the latter case there is a significant spike of similarity within this rather long periplasmic loop. These observations are consistent with the cytoplasmically localised similarity defining NarGH-NarI subunit interactions and a possible electron-transfer conduit. The spike within loop TM4–TM5 may define some other important functionality within NarI, such as a quinol binding site (Q site). Conserved His residues in the NarI sequence correspond to H56 and H66 in TM2, and H187 and H205 of TM5, and their role in haem coordination has been demonstrated by site-directed mutagenesis [58, 60]. In the case of TM5, the two His residues are located on the same segment in a helical wheel projection (fig. 5c). In TM2, the His residues fall in separate segments with approximately 80° between them on the vertical axis, implying that there is a kink in one of the two haem-coordinating helices (most likely in TM5).

The primary location of quinol binding and oxidation appears to be located towards the periplasmic side of NarI (the Q_P site) in close association with haem b_L [58, 60, 63]. However, almost all of the sequence conservation identified in figures 4 and 5 lies towards the cytoplasmic side of the membrane. The exception to this is in the rather long loop between TM4 and TM5. In particular, there is a conserved Trp residue (W162) that appears in all the sequences of figure 4 with the exception of the NarI subunit of *Thermus thermophilus*, where it is replaced by a Tyr residue. Such a highly conserved Trp residue plays an important role in the proximal (Q_P^{FRD}) site of *E. coli* FrdABCD [54, 64] and a number of other Q sites [65]. It is tempting to suggest that this region of the sequence plays a role in defining the Q_P site.

EPR spectroscopy of the two haems

High-level protein overexpression (to $\sim 50\%$ of the inner membrane protein) has allowed intensive scrutiny of the haems of NarGHI in situ in the *E. coli* cytoplasmic membrane [58, 60, 63]. The haems are low-spin (six-coordinate iron) and exhibit EPR spectra with features typical of HALS (highly anisotropic low spin) haems [66], in which there is a large imidazole ligand interplanal angle [67]. In this type of haem, only one of the three g-tensors (g_z) is observed by EPR [68]. Figure 6a shows the deconvoluted EPR spectrum of the two haems, showing features at $g_z = 3.36$ and $g_z = 3.76$. This spectrum is reminiscent of that of the haems *b* of complex III (cytochrome bc_1) [68, 69]. The proposed model for NarI haem coordination (fig. 5b) is similar to that seen in the structure of complex III [70, 71], with the two haems being coordinated between two transmembrane helices. In complex III, the more anisotropic g_z has been assigned to haem b_L, whereas the less anisotropic g_z has been assigned to haem b_H. In mouse complex III, these haems have E_m values of approximately -31 (b_L) and 92 mV (b_H), respectively [72]. In NarGHI, the more anisotropic haem ($g_z = 3.76$; b_H) has an E_m of approximately 120 mV and the less anisotropic haem ($g_z = 3.36$; b_L) has a E_m of approximately 20 mV [58–60].

Site-directed mutagenesis

Assignment of the His ligands of haems b_L and b_H in NarGHI is based on EPR/optical studies of four site-directed mutants, NarGHI[H56R], NarGHI[H66Y], NarGHI[H187Y] and NarGHI[H205Y] [58]. The ligands for haems b_L and b_H are H66/H187 and H56/H205, respectively, in agreement with the sequence conservation of these residues (fig. 4) [62]. This is consistent with the structural model for NarI presented in figure 5b.

Loss of haem b_H in NarGHI[H56R] also significantly modifies some of the remaining prosthetic groups of the enzyme, causing (i) a decrease in the anisotropy (g_z) of haem b_L [58], (ii) an increase in the E_m of haem b_L [60] and (iii) an alteration of the EPR spectrum of the [3Fe–4S] cluster of NarH. The first two observations can be rationalised on the basis that both haems are coordinated between TM2 and TM5 of NarI, and any conformational effects could easily be transferred via these two transmembrane helices. For example, in the cytochrome bc_1 complex, loss of haem b_H also increases the E_m of haem b_L [73]. The effect of the loss of haem b_H on the NarH [3Fe–4S] cluster suggests that this cluster and the haem are located close to the NarH-NarI interface. This is consistent with experimental and structural data on three other enzyme systems. (i) In the crystal structure of *E. coli* FrdABCD [54], the [3Fe–4S] cluster (FR3) of FrdB is located close to the FrdCD-
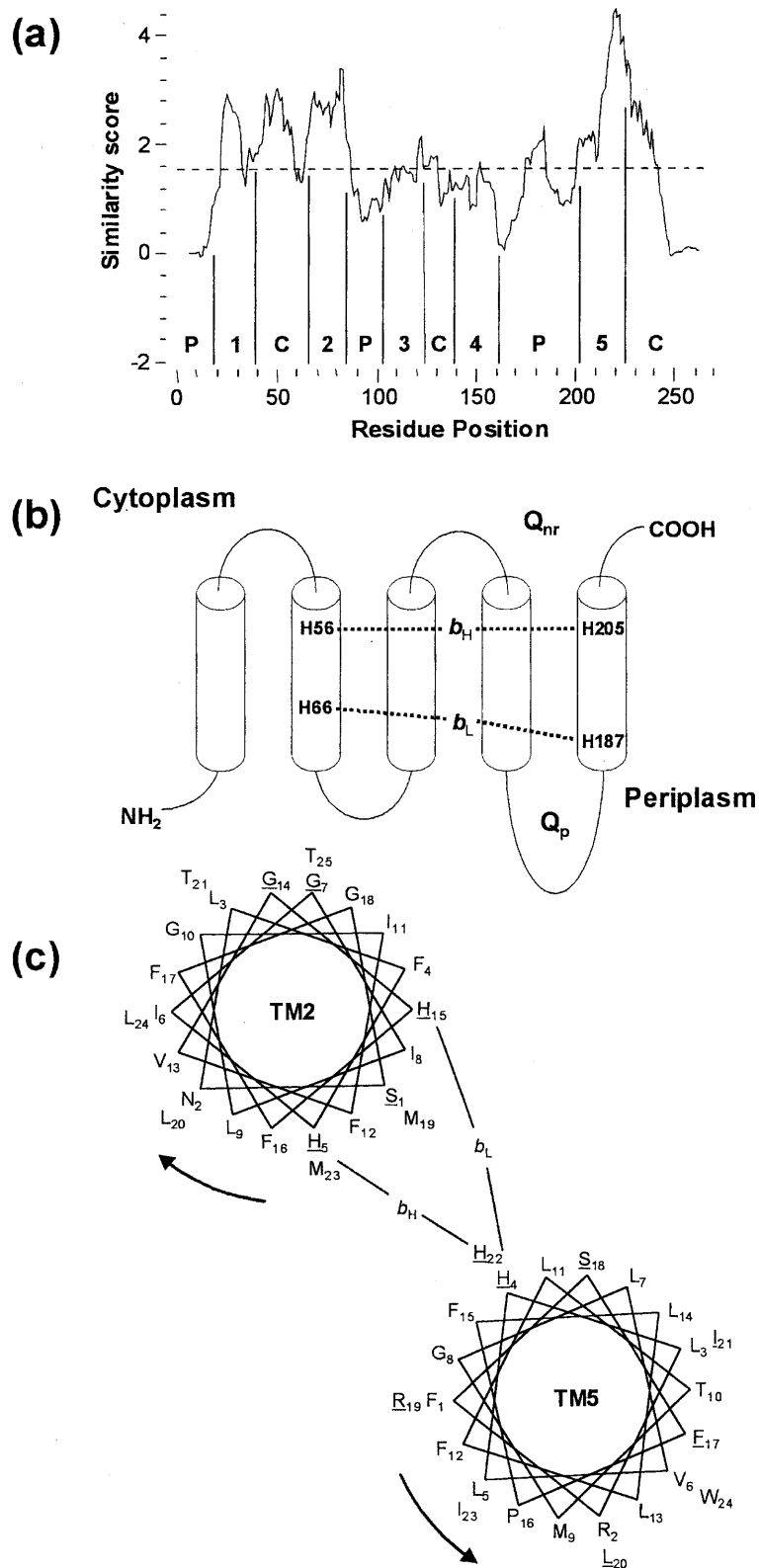
Figure 5. Analyses of the sequence of NarI. (*a*) Plot of sequence similarity versus residue position of the sequence alignment of figure 4 using a window average of 10. The positions of transmembrane segments 1–5 are indicated, as are the proposed locations of the extramembrane loops. The plot was generated using the Plotsimilarity program of the Wisconsin Sequence Analysis Package in combination with the alignment of figure 4. (*b*) Putative transmembrane topology of NarI showing the overall locations of the four conserved His residues involved in haem coordination and the overall locations of the putative Q_P and Q_{nr} quinol binding sites. (*c*) Helical wheel projections of putative transmembrane segments 2 and 5. Shown is the possible view looking away from the NarGH catalytic dimer. Residue numbering is from the start of the putative transmembrane segments identified in figure 4. Absolutely conserved residues are underlined.

FrdB interface. A number of residues of FrdB are located within 5 Å of the proximal MQ binding site (Q_P^{FRD}), and FR3 is located ~ 11 Å from this site. (ii) In *Wollinella succinogenes* fumarate reductase (FrdCAB), the distance between FR3 and the edge of the proximal haem (haem b_P) is also ~ 11 Å [55]. (iii) In *E. coli* DMSO reductase (DmsABC), a [4Fe–4S] cluster of DmsB that is essential for MQH_2 oxidation is located close to a Q site in DmsC (Q_P^{DMS}) and has also been localised close to the DmsB-DmsC interface [74–76]. Thus, in NarGHI, it is possible that haem b_H is in a location similar, relative to the electron-transfer subunit, to the Q_P sites of FrdABCD and DmsABC and the haem b_P of *W. succinogenes* FrdCAB.

When NarI is expressed and assembled into the cytoplasmic membrane in the absence of NarGH [NarI(ΔGH)], its low spin haem EPR spectrum is dramatically altered compared with that of the holoenzyme [58, 60, 63]. The EPR spectrum of NarI(ΔGH) (fig. 6b) exhibits two g_z features attributable to low spin ferric haem, one at $g_z = 3.15$ and another with a $g_z = 2.92$. On the basis of its inhibitor sensitivity, the $g_z = 3.15$ feature can be assigned to haem b_L [63]. The observation of a $g_z = 2.92$ feature may correlate with an almost parallel imidazole ligand orientation [66, 67], indicating that a 'relaxation' in the environment of this haem occurs in the absence of NarGH, as has been observed in the membrane anchors of mitochondrial and *E. coli* succinate dehydrogenase [77, 78]. The $g_z = 2.92$ feature of the spectrum is eliminated in NarI(ΔGH)^{H56R}, unequivocally assigning it to a 'relaxed' form of haem b_H. The E_m of haem b_L in NarI(ΔGH) is 37 mV, which is a modest increase from the value of $+20$ observed in NarGHI [60]. Surprisingly, the E_m of haem b_H drops from $+120$ mV in NarGHI to -178 mV in NarI(ΔGH), a change of almost -300 mV. In chloroplast cytochrome b_{559}, exposure of the haem to the aqueous milieu results in a similar drop in E_m [79], suggesting that the absence of the NarGH results in a similar exposure of haem b_H in NarI(ΔGH). This is further evidence for the localisation of haem b_H to the NarH–NarI interface region of NarGHI.

Q-site inhibitors

NarGHI is able to use both menaquinol (MQH_2) and ubiquinol (UQH_2) as physiological reductants [46, 80, 81]. Significant progress in studies of quinol binding has been made using quinol analogue substrates and inhibitors in combination with optical, fluorescence and EPR spectroscopies. Of a range of Q-site inhibitors of complex III tested [63], only HOQNO and stigmatellin inhibit NarGHI with a sufficiently low concentration for them to be useful for further biochemical/biophysical studies. HOQNO binding to NarGHI renders haem

b_L more anisotropic (g_z increases to ~ 3.50), suggesting that it increases the imidazole ligand interplanal angle [60, 63, 66]. Stigmatellin also binds in the vicinity of haem b_L, but in this case there is a decrease in anisotropy, suggesting a decrease in the imidazole ligand interplanal angle. These different responses correlate well with the effects of the two inhibitors on the haem E_m values. HOQNO causes a near reversal of the E_m values (a positive ΔE_m for haem b_L and a negative ΔE_m for haem b_H), whereas stigmatellin elicits a modest positive ΔE_m on haem b_L and has no effect on haem b_H [60]. Overall, these results suggest the presence of a dissociable Q site (the Q_P site) in the vicinity of haem
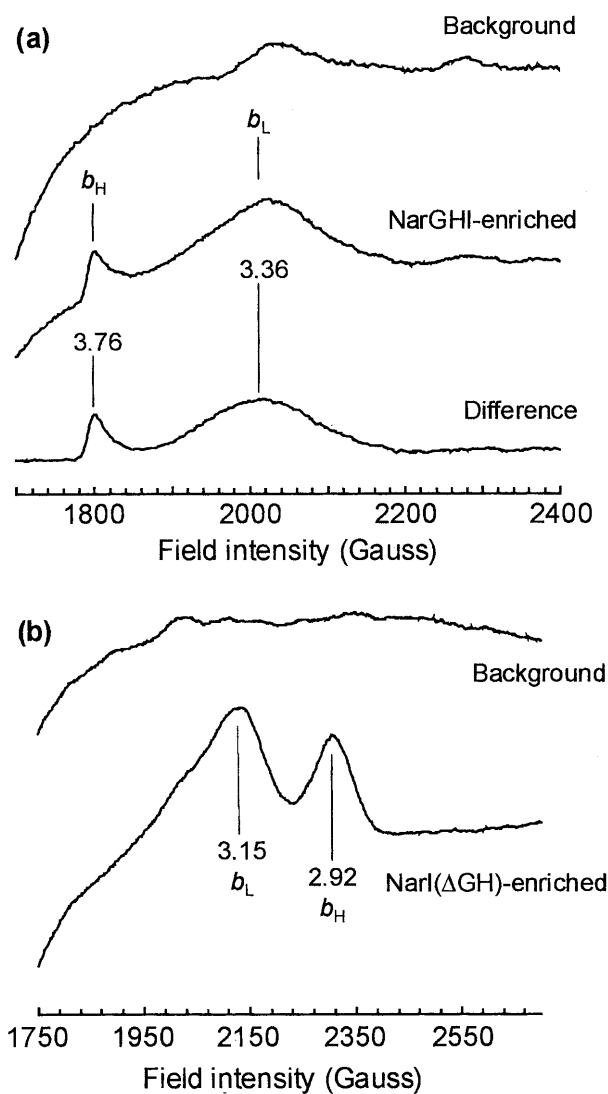

Figure 6. EPR spectra of NarGHI (*a*) and NarI(ΔGH) (*b*) in *E. coli* inner membranes. Spectra were recorded at a temperature of 12 K with a modulation amplitude of 20 G_{pp} at a microwave power of 20 mW for (*a*) and 2 mW for (*b*).

b_L. The negative ΔE_m elicited by HOQNO on haem b_H suggests either that a conformational change is propagated to this haem via the haem b_L and TM2/TM5, or that there is another site of HOQNO binding in the vicinity of haem b_H.

The determination of the number of dissociable HOQNO binding sites (and presumably MQH_2 binding sites) was achieved through the use of fluorescence quench titrations [82–84]. Binding to NarGHI occurs with a K_d of ~ 0.2 μM at a single site that is sensitive to the absence of haem b_L, but not to the absence of haem b_H [60]. This site appears to overlap with, or be sterically hindered by, the site for stigmatellin binding. The absence of NarGH in NarI(ΔGH) does not appear to affect HOQNO binding. Thus, a combination of EPR and fluorescence spectroscopies points to a model for quinol binding in which there is a single dissociable high-affinity site (the Q_P site) located towards the periplasmic side of NarI in close proximity to haem b_L. This model is consistent with the proposed bioenergetics of NarGHI in which scalar protons from MQH_2 oxidation are released into the periplasm during enzyme turnover [85, 62].

There is evidence suggesting that a second Q site exists in NarGHI (the Q_{nr} site). During nitrate-induced enzyme turnover, an HOQNO-sensitive radical species is observed that is likely to be located in the vicinity of the NarH [3Fe–4S] cluster [54]. It has been proposed that this species is a menasemiquinone anion that arises from a tightly bound MQ-9 that copurifies with the NarGH catalytic dimer [52, 86]. Also, HOQNO and stigmatellin inhibit nitrate-dependent haem reoxidation [63] (fig. 7), suggesting the presence of a second dissociable Q site between haem b_H and the [3Fe–4S] cluster (the Q_{nr} site). This site would perhaps be similar to the Q_P^{FRD} [56] and Q_P^{DMS} [74–76] sites. However, in contrast with what is observed with FrdABCD [87, 88], HOQNO elicits no effect on the [3Fe–4S] cluster of NarH [60]. It is possible that the observed inhibition of haem reoxidation in NarGHI is due to bound inhibitor (at the Q_P site) preventing oxidation of haem b_L (in the case of HOQNO, the ΔE_m elicited on haem b_L is entirely consistent with this possibility). It should also be noted that the presence of a dissociable Q_{nr} site would be difficult to reconcile with the proposed bioenergetics of NarGHI [85, 62]. When quinol-dependent haem reduction is followed optically in the presence of HOQNO or stigmatellin (fig. 7), it is clear that there is less inhibition observed than when haem oxidation in the presence of inhibitor is followed, suggesting that HOQNO and stigmatellin bind with higher affinity to the reduced form of NarGHI.

Quinol binding and oxidation by NarGHI has also been addressed by steady-state enzymology. When the hydroxylated naphthoquinols reduced lapachol and plumbagin are used as substrates, kinetics are observed that are consistent with binding to a single site within the
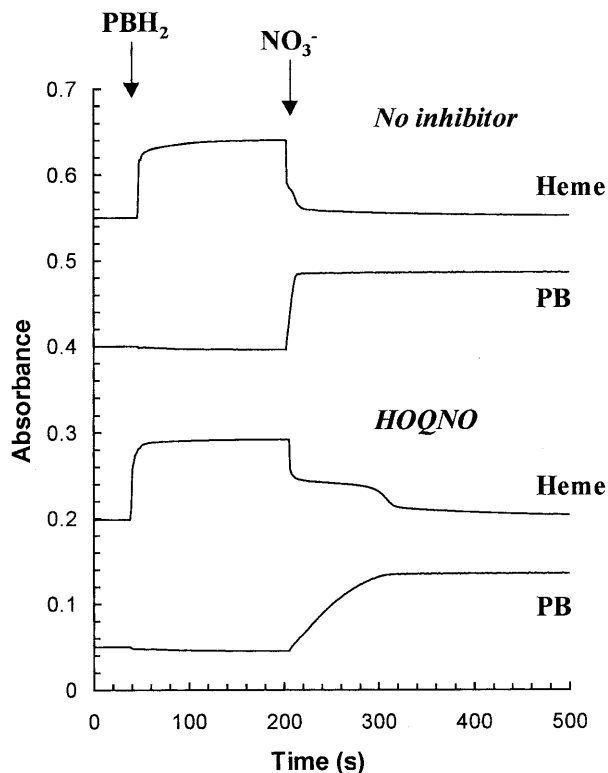

Figure 7. Use of reduced plumbagin to follow haem and quinol redox states in the presence of HOQNO. Membranes enriched in NarGHI (0.6 mg ml^{-1} of protein) were incubated in N_2-saturated 100 mM MOPS/5 mM EDTA (pH 7.0). 0.345 mM final concentration reduced plumbagin (PBH$_2$) was added, and the reduction of the haems was followed by measuring the OD$_{560-575}$ ($\times 1.0$). The redox state of the PBH$_2$ was measured by following the OD$_{419-575}$ ($\times 0.05$). Subsequent oxidation was accomplished by adding 17 mM KNO$_3$. (a) and (b), traces in the absence of HOQNO. (c) and (d), traces in the presence of 34 μM HOQNO.

NarGHI complex [81]. However, a more complex analysis [89] suggested the presence of two quinol binding sites, one which preferentially binds a MQH_2 analogue and another which preferentially binds a UQH_2 analogue (i.e. the data suggest two sites for both MQH_2 and UQH_2 analogues). However, in another steady-state kinetics study [90], the data were consistent with only a single dissociable Q site (for UQH_2). Thus, at the present time, not all the kinetic data agree with the EPR/fluorescence data suggesting only a single Q site in the vicinity of haem b_L.

In the context of identifying the number of Q sites in NarGHI, it is important to distinguish between dissociable and nondissociable sites. For example, the MQ-9 identified in purified NarGHI dimer [86] could reside at a nondissociable Q site in a position equivalent to the proposed Q_{nr} site. Such a nondissociable quinol species has been identified in E. coli cytochrome bo [91–93] as

well as in the well-characterised bacterial photoreaction centre (the so-called Q_A site) [94, 95]. Thus, the absolute determination of the number of Q sites in NarGHI requires additional intensive investigation.

Summary and questions for future directions

No three-dimensional structure is available for Nar-GHI-type enzymes, but the extensive blocks of homology throughout the length of NarG with those of proteins with known structures strongly suggests that NarG subunit is also organised in four domains around the molybdenum cofactor. The increasing speed with which crystal structures of multimeric proteins are reported allows us to hope that the 3D structure of a membrane-bound nitrate reductase will soon be available. While we have learned much about the type and the coordination of the redox centres of membrane-bound nitrate reductases, there are several interesting and important questions still to be answered. The field is now moving from a period of redox-centre characterisation to understanding how they are integrated into the electron pathway. In the light of recent publications on metalloenzyme maturation, it appears that we are also entering a new area in which more emphasis will be placed on understanding how the individual subunits are integrated into a functional complex. A cascade of several protein-protein interactions seems to be involved in these processes mediated by accessory proteins and specific chaperones. Their understanding will be one of the most exciting fields during the next decade.

1 Blasco F., Iobbi C., Giordano G., Chippaux M. and Bonnefoy V. (1989) Nitrate reductase of *Escherichia coli*: completion of the nucleotide sequence of the *nar* operon and reassessment of the role of the alpha and beta subunits in iron binding and electron-transfer. Mol. Gen. Genet. **281:** 249–256

2 Grove J., Tanapongpipat S., Thomas G., Griffiths L., Crooke H. and Cole H. (1996) *Escherichia coli* K-12 genes essential for the synthesis of c-type cytochromes and a third nitrate reductase located in the periplasm. Mol. Microbiol. **19:** 467–481

3 Blasco F., Iobbi C., Ratouchniak J., Bonnefoy V. and Chippaux M. (1990) Nitrate reductases of *Escherichia coli*: sequence of the second nitrate reductase and comparison with that encoded by the *narGHJI* operon. Mol. Gen. Genet. **222:** 104–111

4 Bonnefoy V. and DeMoss J. A. (1994) Nitrate reductases in *Escherichia coli*. Antonie Van Leeuwenhoek **66:** 47–56

5 Iobbi C., Santini C. L., Bonnefoy V. and Giordano G. (1987) Biochemical and immunological evidence for a second nitrate reductase in *Escherichia coli* K12. Eur. J. Biochem. **168:** 451–459

6 Chang L., Wei L. I., Morton R. A. and Schellhorn H. E. (1999) Expression of the *Escherichia coli* NRZ nitrate reductase is highly growth phase dependent and is controlled by RpoS, the alternative vegetative sigma factor. Mol. Microbiol. **34:** 756–766

7 Potter L. C. and Cole J. A. (1999) Essential roles for the products of the *napABCD* genes, but not *napFGH*, in periplasmic nitrate reduction by *Escherichia coli* K-12. Biochem. J. **344:** 69–76

8 Potter L. C., Millington P., Thomas G. H. and Cole J. A. (1999) Competition between *Escherichia coli* strains expressing either a periplasmic or a membrane-bound nitrate reductase: does Nap confer a selective advantage during nitrate-limited growth? Biochem. J. **344:** 77–84

9 Wang H., Tseng C. and Gunsalus R. P. (1999) The *napF* and *narG* nitrate reductase operons in *Escherichia coli* are differentially expressed in response to submicromolar concentrations of nitrate but not nitrite. J. Bacteriol. **181:** 5303–5308

10 Schindelin H., Kisker C., Hilton J., Rajagopalan K. V. and Rees D. C. (1996) Crystal structure of DMSO reductase: redox-linked changes in molybdopterin coordination. Science **272:** 1615–1621

11 Schneider F., Lowe J., Huber R., Schindelin H., Kisker C. and Knabelin J. (1996) Crystal structure of dimethyl sulfoxide reductase from *Rhodobacter capsulatus* at 1.88 Å resolution. J. Mol. Biol. **263:** 53–69

12 Boyington J. C., Gladyshev V. N., Khangulov S. V., Stadtman T. C. and Sun P. D. (1997) Crystal structure of formate dehydrogenase H: catalysis involving Mo, molybdoprotein, selenocysteine and an Fe4S4 cluster. Science **275:** 1305–1308

13 Czjzek M., Dos Santos J.-P., Pommier J., Giordano G., Méjean V. and Haser R. (1998) Crystal structure of oxidized trimethylamine N-oxide reductase from *Shewanella massilia* at 2.5 Å resolution. J. Mol. Biol. **284:** 435–447

14 Dias J. M., Than E., Humm A., Huber R., Bourenkov G. P., Bartunik H. D. et al. (1999) Crystal structure of the first dissimilatory nitrate reductase at 1.9 Å solved by MAD methods. Structure **7:** 65–79

15 Berks B. C., Ferguson S. J., Moir J. W. and Richardson D. J. (1995) Enzymes and associated electron transport systems that catalyse the respiratory reduction of nitrogen oxides and oxyanions. Biochim. Biophys. Acta **1232:** 97–173

16 Wootton J. C., Nicolson R. E., Cock J. M., Walters D. E., Burke J. F., Doyle W. A. et al. (1991) Enzymes depending on the pterin molybdenum cofactor: sequence families, spectroscopic properties of molybdenum and possible cofactor-binding domains. Biochim. Biophys. Acta **1057:** 157–185

17 Trieber C. A., Rothery R. A. and Weiner J. H. (1996) Engineering a novel iron-sulfur cluster into the catalytic subunit of *Escherichia coli* dimethyl-sulfoxide reductase. J. Biol. Chem. **271:** 4620–4626

18 Volbeda A., Charon M. H., Piras C., Hatchikian E. C., Frey M. and Fontecilla-Camps J. C. (1995) Crystal structure of the nickel-iron hydrogenase from *Desulfovibrio gigas*. Nature **373:** 580–587

19 Magalon A., Asso M., Guigliarelli B., Rothery R. A., Bertrand P., Giordano G. et al. (1998) Molybdenum cofactor properties and [Fe-S] cluster coordination in *Escherichia coli* nitrate reductase A: investigation by site-directed mutagenesis of the conserved is-50 residue in the NarG subunit. Biochemistry **37:** 7363–7370

20 Rothery R. A., Trieber C. A. and Weiner J. H. (1999) Interactions between the molybdenum cofactor and iron-sulfur clusters of *Escherichia coli* dimethylsulfoxide reductase. J. Biol. Chem. **272:** 13002–13009

21 Trieber C. A., Rothery R. A. and Weiner J. H. (1994) Multiple pathways of electron-transfer in dimethyl sulfoxide reductase of *Escherichia coli*. J. Biol. Chem. **269:** 7103–7109

22 Hille R. (1996) The mononuclear molybdenum enzymes. Chem. Rev. **96:** 2757–2816

23 Vincent S. P. and Bray R. C. (1978) Electron-paramagnetic-resonance studies on nitrate reductase from *Escherichia coli* K12. Biochem. J. **171:** 639–647

24 Godfrey C., Greenwood C., Thomson A. J., Bray R. C. and George G. N. (1984) Electron-paramagnetic-resonance spectroscopy studies on the dissimilatory nitrate reductase from *Pseudomonas aeruginosa*. Biochem. J. **224:** 601–608

25 Sodergren E. J., Hsu P. Y. and DeMoss J. A. (1988) Roles of the *narJ* and *narI* gene products in the expression of nitrate reductase in *Escherichia coli*. J. Biol. Chem. **263:** 16156–16162

26 Blasco F., Pommier J., Augier V., Chippaux M. and Giordano G. (1992) Involvement of the *narJ* or *narW* gene product in the formation of active nitrate reductase in *Escherichia coli*. Mol. Microbiol. **6:** 221–230

27 Palmer T., Santini C. L., Iobbi-Nivol C., Eaves D. J., Boxer D. H. and Giordano G. (1996) Involvement of the *narJ* and *mob* gene products in distinct steps in the biosynthesis of the molybdoenzyme nitrate reductase in *Escherichia coli*. Mol. Microbiol. **20:** 875–884

28 Blasco F., Dos Santos J. P., Magalon A., Frixon C., Guigliarelli B., Santini C. L. et al. (1998) NarJ is a specific chaperone required for molybdenum cofactor assembly in nitrate reductase A of *Escherichia coli*. Mol. Microbiol. **28:** 435–447

29 Hoffmann T., Troup B., Szabo A., Hungerer C. and Jahn D. (1995) The anaerobic life of *Bacillus subtilis*: cloning of the genes encoding the respiratory nitrate reductase system. FEMS Microbiol. Lett. **131:** 219–225

30 Ramirez-Arcos S., Fernandez-Herrero L. A. and Berenguer J. (1998) A thermophilic nitrate reductase is responsible for the strain specific anaerobic growth of *Thermus thermophilus* HB8. Biochem. Biophys. Acta **1396:** 215–227

31 Liu X. and DeMoss J. A. (1997) Characterization of NarJ, a system-specific chaperone required for nitrate reductase biogenesis in *Escherichia coli*. J. Biol. Chem. **272:** 24266–24271

32 Rothery R. A., Magalon A., Giordano G., Guigliarelli B., Blasco F. and Weiner J. H. (1998) The molybdenum cofactor of *Escherichia coli* nitrate reductase A (NarGHI). Effect of a *mobAB* mutation and interactions with [Fe-S] clusters. J. Biol. Chem. **273:** 7462–7469

33 Amy N. K. and Rajagopalan K. V. (1979) Characterization of molybdenum cofactor from *Escherichia coli*. J. Bacteriol. **140:** 114–124

34 Giordano G., Santini C. L., Saracino L. and Iobbi C. (1987) Involvement of a protein with molybdenum cofactor in the in vitro activation of nitrate reductase from a *chlA* mutant of *Escherichia coli* K12. Biochem. Biophys. Acta **914:** 220–232

35 Park I. S., Carr M. B. and Hausinger R. P. (1994) In vitro activation of urease apoprotein and role of UreD as a chaperone required for nickel metallocenter assembly. Proc. Natl. Acad. Sci. USA **91:** 3233–3237

36 Drapal N. and Bock A. (1998) Interaction of the hydrogenase accessory protein HypC with HycE, the large subunit of *Escherichia coli* hydrogenase 3 during enzyme maturation. Biochemistry **37:** 2941–2948

37 Pommier J., Méjean V., Giordano G. and Iobbi-Nivol C. (1998) TorD, a cytoplasmic chaperone that interacts with the unfolded trimethylamine N-oxide reductase enzyme (TorA) in *Escherichia coli*. J. Biol. Chem. **273:** 16615–16620

38 Leimkühler S. and Klipp W. (1999) Role of XdhC in molybdenum cofactor insertion into xanthine dehydrogenase of *Rhodobacter capsulatus*. J. Bacteriol. **181:** 2745–2751

39 Berg B. L., Li J., Heider J. and Stewart V. (1991) Nitrate-inducible formate dehydrogenase in *Escherichia coli* K-12. I. Nucleotide sequence of the *fdnGHI* operon and evidence that opal (UGA) encodes selenocysteine. J. Biol. Chem. **266:** 22380–22385

40 Bilous P. T., Cole S. T., Anderson W. F. and Weiner J. H. (1988) Nucelotide sequence of the *dmsABC* operon encoding the anaerobic dimethylsulfoxide reductase of *Escherichia coli*. Mol. Microbiol. **2:** 785–795

41 Plunkett G., 3d, Burland V., Daniels D. L., Blattner F. R. (1993) Analysis of the *Escherichia coli* genome. III. DNA sequence of the region from 87.2 to 89.2 minutes. Nucleic. Acids Res. **21:** 3391–3398

42 Krafft T., Bokranz M., Klimmek O., Schroder I., Fahrenholz F., Kojro E. et al. (1992) Cloning and nucleotide sequence of the *psrA* gene of *Wolinella succinogenes* polysulphide reductase. Eur. J. Biochem. **206:** 503–510

43 Guigliarelli B., Asso M., More C., Augier V., Blasco F., Pommier J. et al. (1992) EPR and redox characterization of iron-sulfur centers in nitrate reductases A and Z from *Escherichia coli*. Evidence for a high-potential and a low-potential class and their relevance in the electron-transfer mechanism. Eur. J. Biochem. **207:** 61–68

44 More C., Camensuli P., Dole F., Guigliarelli B., Asso M., Fournel A. et al. (1996) A new approach for the structural study of metalloproteins: the quantitative analysis of intercenter magnetic interactions. J. Biol. Inorg. Chem. **1:** 152–161

45 Augier V., Asso M., Guigliarelli B., More C., Bertrand P., Santini C. L. et al. (1993) Removal of the high-potential [4Fe-4S] center of the beta-subunit from *Escherichia coli* nitrate reductase. Physiological, biochemical and EPR characterization of site-directed mutated enzymes. Biochemistry **32:** 5099–5108

46 Guigliarelli B., Magalon A., Asso M., Bertrand P., Frixon C., Giordano G. et al. (1996) Complete coordination of the four Fe-S centers of the beta subunit from *Escherichia coli* nitrate reductase. Physiological, biochemical and EPR characterization of site-directed mutants lacking the highest or lowest potential [4Fe-4S] clusters. Biochemistry **35:** 4828–4836

47 Augier V., Guigliarelli B., Asso M., Bertrand P., Frixon C., Giordano G. et al. (1993) Site-directed mutagenesis of conserved cysteine residues within the beta subunit of *Escherichia coli* nitrate reductase. Physiological, biochemical and EPR characterization of the mutated enzymes. Biochemistry **32:** 2013–2023

48 Stout C. D. (1988) 7-iron ferredoxin revisited. J. Biol. Chem. **263:** 9256–9260

49 Guigliarelli B. and Bertrand P. (1999) Application of EPR spectroscopy to the structural and functional study of iron-sulfur proteins. Adv. Inorg. Chem. **47:** 421–497

50 Mehari T., Qiao F., Scott M. P., Nellis D. F., Zhao J., Bryant D. A. et al. (1995) Modified ligands to FA and FB in photosystem I. I. Structural constraints for the formation of iron-sulfur clusters in free and rebound PsaC. J. Biol. Chem. **270:** 108–117

51 Golbeck J. H. (1999) A comparative analysis of the spin state distribution of in vitro and in vivo mutant of PsaC. Photosynthesis Res. **61:** 107–144

52 Magalon A., Rothery R. A., Giordano G., Blasco F. and Weiner J. H. (1997) Characterization by electron paramagnetic resonance of the role of the *Escherichia coli* nitrate reductase (NarGHI) iron-sulfur clusters in electron-transfer to nitrate and identification of a semiquinone radical intermediate. J. Bacteriol. **179:** 5037–5045

53 Philippot L. and Hojberg O. (1999) Dissimilatory nitrate reductase in bacteria. Biochim. Biophys. Acta **1446:** 1–23

54 Iverson T. M., Luna-Chavez C., Cecchini G. and Rees D. C. (1999) Structure of *Escherichia coli* fumarate reductase respiratory complex. Science **284:** 1961–1966

55 Lancaster C. R. D., Kröger A., Auer M. and Michel H. (1999) Structure of fumarate reductase from *Wolinella succinogenes* at 2.2 Å resolution. Nature **402:** 377–385

56 Rousset M., Montet Y., Guigliarelli B., Forget N., Asso M., Bertrand P. et al. (1998) [3Fe-4S] to [4Fe-4S] cluster conversion in *Desulfovibrio fructosovorans* [NiFe] hydrogenase by site-directed mutagenesis. Proc. Natl. Acad. Sci. USA **95:** 11625–11630

57 Page C. C., Moser C. C., Chen X. and Dutton P. L. (1999) Natural engineering principles of electron tunnelling in biological oxidation-reduction. Nature **402:** 47–52

58 Magalon A., Lemesle-Meunier D., Rothery R. A., Frixon C., Weiner J. H. and Blasco F. (1997) Heme axial ligation by the highly conserved His residues in helix II of cytochrome b (NarI) of *Escherichia coli* nitrate reductase A. J. Biol. Chem. **272:** 25652–25658

59 Hackett N. R. and Bragg P. D. (1982) The association of two distinct b cytochromes with the respiratory nitrate reductase of *Escherichia coli*. FEBS Microbiol. Lett. **13**: 213–217

60 Rothery R. A., Blasco F., Magalon A., Asso M. and Weiner J. H. (1999) The hemes of *Escherichia coli* nitrate reductase A (NarGHI): potentiometric effects of inhibitor binding to NarI. Biochemistry **38**: 12748–12757

61 Thompson J. D., Higgings D. G. and Gibson T. J. (1994) CLUSTAL W: improving the sensitivity of progressive multiple sequence alignment through sequence weighting, position-specific gap penalties and weight matrix choice. Nucleic Acids Res. **22**: 4673–4680

62 Berks B. C., Page M. D., Richardson D. J., Reilly A., Cavill A., Outen F. et al. (1995) Sequence analysis of subunits of the membrane-bound nitrate reductase from a denitrifying bacterium: the integral membrane subunit provides a prototype for the dihaem electron-carrying arm of a redox loop. Mol. Microbiol. **15**: 319–331

63 Magalon A., Rothery R. A., Lemesle-Meunier D., Frixon C., Weiner J. H. and Blasco F. (1998) Inhibitor binding within the NarI subunit (cytochrome bnr) of *Escherichia coli* nitrate reductase A. J. Biol. Chem. **273**: 10851–10856

64 Westenberg D. J., Gunsalus R. P., Ackrell B. A., Sices H. and Cecchini G. (1993) *Escherichia coli* fumarate reductase frdC and frdD mutants. Identification of amino acid residues involved in catalytic activity with quinones. J. Biol. Chem. **268**: 815–822

65 Murray L., Pires R. H., Hastings S. F. and Ingledew W. J. (1999) Models for structure and function in quinone binding sites: the *Escherichia coli* quinol oxidase, cytochrome *bo3*. Biochem. Soc. Trans. **27**: 581–585

66 Walker F. A., Huynh B. H., Scheidt W. R. and Osvarth S. R. (1986) Models of the cytochromes b. Effect of axial ligand plane orientation on the EPR and Mossbauer spectra of low-spin ferrihemes. J. Am. Soc. Trans. **108**: 5288–5297

67 Dou Y., Admiraal S. J., Ikeda-Saito M., Krzywda S., Wilkinson A. J., Li T. et al. (1995) Alteration of axial coordination by protein engineering in myoglobin. Bisimidazole ligation in the His64→Val/Val68→His double mutant. J. Biol. Chem. **270**: 15993–16001

68 Salerno J. C. (1984) Cytochrome electron spin resonance line, ligand fields and components stoichiometry in ubiquinol-cytochrome c oxidoreductase. J. Biol. Chem. **259**: 2331–2336

69 Valkova-Valchanova M. B., Saribas A. S., Gibney B. R., Dutton P. L. and Daldal F. (1998) Isolation and characterization of a two-subunit cytochrome bc1 subcomplex from *Rhodobacter capsulatus* and reconstitution of its ubihydroquinone oxidation (Qo) site with purified Fe-S protein subunit. Biochemistry **37**: 16242–16251

70 Zhang Z., Huang L., Shulmeister V., Chi Y., Kim K. K., Hung L. et al. (1998) Electron-transfer by domain movement in cytochrome bc1. Nature **392**: 677–684

71 Xia D., Yu C.-A., Kim H., Xia J.-Z., Kachurin A. M., Zhang L. et al. (1997) Crystal structure of the cytochrome bc₁ complex from bovine heart mitochondria. Science **277**: 60–66

72 Howell N. and Robertson D. E. (1993) Electrochemical and spectral analysis of the long-range interactions between the Qo and Qi sites and the heme prosthetic groups in ubiquinol-cytochrome c oxidoreductase. Biochemistry **32**: 11162–11172

73 Yun C. H., Crofts A. R. and Gennis R. B. (1991) Assignment of the histidine axial ligands to the cytochrome b$_H$ and cytochrome b$_L$ components of the bc₁ complex from *Rhodobacter sphaeroides* by site-directed mutagenesis. Biochemistry **30**: 6747–6754

74 Rothery R. A. and Weiner J. H. (1991) Alteration of the iron-sulfur cluster composition of *Escherichia coli* dimethyl sulfoxide reductase by site-directed mutagenesis. Biochemistry **30**: 8296–8305

75 Rothery R. A. and Weiner J. H. (1993) Topological characterization of *Escherichia coli* DMSO reductase by electron paramagnetic resonance spectroscopy of an engineered [3Fe-4S] cluster. Biochemistry **32**: 5855–5861

76 Rothery R. A. and Weiner J. H. (1996) Interaction of an engineered [3Fe-4S] cluster with a menaquinol binding site of *Escherichia coli* DMSO reductase. Biochemistry **35**: 3247–3257

77 Yu L., Xu J.-X., Haley P. E. and Yu C.-A. (1987) Properties of bovine heart mitochondrial cytochrome *b560*. J. Biol. Chem. **262**: 1137–1143

78 Yang X., Yu L. and Yu C. A. (1997) Resolution and reconstitution of succinate-ubiquinone reductase from *Escherichia coli*. J. Biol. Chem. **272**: 9683–9689

79 Krishtalik L. I., Tae G.-S., Cherepanov D. A. and Cramer W. A. (1993) The redox properties of cytochromes b imposed by the membrane electrostatic environment. Biophys. J. **65**: 184–195

80 Wallace B. J. and Young I. G. (1977) Role of quinones in electron transport to oxygen and nitrate in *Escherichia coli*. Studies with a *ubiA*- *menA*- double quinone mutant. Biochim. Biophys. Acta **461**: 84–100

81 Rothery R. A., Chatterjee I., Kiema G., McDermott M. T. and Weiner J. H. (1998) Hydroxylated naphthoquinones as substrates for *Escherichia coli* anaerobic reductases. Biochem. J. **332**: 35–41

82 Brandt U. and von Jagow G. (1991) Analysis of inhibitor binding to the mitochondrial cytochrome c reductase by fluorescence quench titration. Evidence for a 'catalytic switch' at the Qo center. Eur. J. Biochem. **195**: 163–170

83 Okun J. G., Lümmen P. and Brandt U. (1999) Three classes of inhibitors share a common binding domain in mitochondrial complex I (NADH:ubiquinone oxidoreductase). J. Biol. Chem. **274**: 2626–2630

84 van Ark G. and Berden J. A. (1977) Binding of HOQNO to beef-heart submitochondrial particles. Biochim. Biophys. Acta **459**: 119–137

85 Jones R. W., Lamont A. and Garland P. B. (1980) The mechanism of proton translocation driven by the respiratory nitrate reductase complex of *Escherichia coli*. Biochem. J. **190**: 79–94

86 Brito F., DeMoss J. A. and Dubourdieu M. (1995) Isolation and identification of menaquinone-9 from purified nitrate reductase of *Escherichia coli*. J. Bacteriol. **177**: 3728–3735

87 Rothery R. A. and Weiner J. H. (1998) Interaction of a menaquinol binding site with the [3Fe–4S] cluster of *Escherichia coli* fumarate reductase. Eur. J. Biochem. **254**: 588–595

88 Hägerhäll C., Magnitsky S., Sled V. D., Schröder I., Gunsalus R. P., Cecchini G. et al. (1999) An *Escherichia coli* mutant quinol: fumarate reductase contains an EPR-detectable semiquinone stabilized at the proximal quinone binding site. J. Biol. Chem. **274**: 26157–26164

89 Giordani R., Buc J., Cornish-Bowden A. and Cardenas M.-L. (1997) Kinetic studies of membrane-bound nitrate reductase A from *Escherichia coli* with menadiol and duroquinol, analogues of physiological electron donors. Eur. J. Biochem. **250**: 567–577

90 Morpeth F. F. and Boxer D. H. (1985) Kinetic analysis of respiratory nitrate reductase from *Escherichia coli* K12. Biochemistry **24**: 40–46

91 Ingledew W. J., Ohnishi T. and Salerno J. C. (1995) Studies on a stabilisation of ubisemiquinone by *Escherichia coli* quinol oxidase, cytochrome bo. Eur. J. Biochem. **227**: 903–908

92 Sato-Watanabe M., Mogi T., Ogura T., Kitagawa T., Miyoshi H., Iwamura H. et al. (1994) Identification of a novel quinone-binding site in the cytochrome bo complex from *Escherichia coli*. J. Biol. Chem. **269**: 28908–28912

93 Sato-Watanabe M., Itoh S., Mogi T., Matsuura K., Miyoshi H. and Anraku Y. (1995) Stabilization of a semiquinone radical at the high-affinity quinone binding site (QH) of the *Escherichia coli* bo-type ubiquinol oxidase. FEBS Lett. **374**: 265–269

94 Ermler U., Michel H. and Schiffer M. (1994) Structure and function of the photosynthetic reaction center from *Rhodobacter sphaeroides*. J. Bioenerget. Biomem. **26**: 5–15

95 Allen J. P. and Williams J. C. (1998) Photosynthetic reaction centers. FEBS Lett. **438**: 5–9